

# THE SCANNING MECHANISM FOR ROSETTA / MIDAS FROM AN ENGINEERING MODEL TO THE FLIGHT MODEL

R. Le Letty <sup>(1)</sup>, F. Barillot <sup>(1)</sup>, N. Lhermet <sup>(1)</sup>, F. Claeysen <sup>(1)</sup>, M. Yorck <sup>(2)</sup>, J. Gavira Izquierdo <sup>(3)</sup>, H. Arends <sup>(3)</sup>

(1) CEDRAT RECHERCHE, 10, ch. de Pré Carré, ZIRST, F38246 Meylan, France, Phone : +33.4.76.90.50.45, Fax : +33.4.76.90.16.09., [actuator@cedrat.com](mailto:actuator@cedrat.com)

(2) ATOS origin BV, Haagse Showweg 6G, 2332KG, Leiden, The Netherlands,

(3) ESA/ESTEC, Keplerlaan 1, 2201AZ, Noordwijk, The Netherlands.

## 1 Abstract

The MIDAS (Micro Imaging Dust Analysis System) [1] instrument jointly developed by IWF Graz (AT) and the Solar Space Division of ESA/ESTEC (NL) will flow on ROSETTA and will analyse the dust of the 46P/Wirtanen cometa using an Atomic Force Microscope (AFM). A piezoelectric XYZ stage, used to scan the sample in 3 axis, is part of the instrument and has been fully designed and qualified under the ESA/ESTEC contract n°13090/98/NL/MV. Two qualification models (EQM / QM) and two flight models (FM / FSM) have been integrated and fully tested within 18 months (Figure 1).

The basic principle of the stage has been described in a previous paper [2]. The XY stage includes a latch mechanism based on two Shape Memory actuators. This paper focuses on the lessons learned during the qualification campaign, especially on the testing activities and on the latch mechanism.

The XYZ stage has followed a full qualification campaign including Thermal Vacuum cycles, Random Vibrations tests and lifetime tests. The latch mechanism has been designed and tested with the following features :

- easiness of locking and refurbishment operations,
- compatibility with the parallel two degrees of freedom mechanism,
- low shock device.

It has been tested more than 20 times, including 4 tests in the worst case conditions (eg the most demanding power case at  $-20^{\circ}\text{C}$ ) and 2 times after a vibration test. The results and the parameters influencing the reproducibility are discussed.

The functional performances have been assessed using a dedicated test bench. Comments are made on the measurements techniques used to get results independent from the drift effect displayed by the piezo components.

The calibration work (static and gain of the position sensors) have played an important role during the testing activities. Several parameters (temperature, piezo drift effect and external forces acting on the stage and coming from the coarse approach mechanism) affects the static position. Because of the limited stroke range of reading of the capacitive sensors, some

adjustments works have become necessary after the integration in the MIDAS instrument.

The four identical models (EQM, QM, FM, FSM) have brought useful data for future piezo mechanisms, both on the integration's reproducibility and on the measurement techniques accuracy.

## 2 General design

### 2.1 Description

The whole mechanism has a total mass of 510 gr and includes 110 parts. The XY stage has an asymmetric configuration and use 8 amplified piezoelectric actuators APA50S [3]. The guiding is ensured by some elastic flexural hinges (Figure 5). The X and Y channel are monitored by capacitive sensors. The Z actuator is a direct prestressed actuator equipped with a full Wheastone bridge of Strain Gauges and mounted on the moving frame.

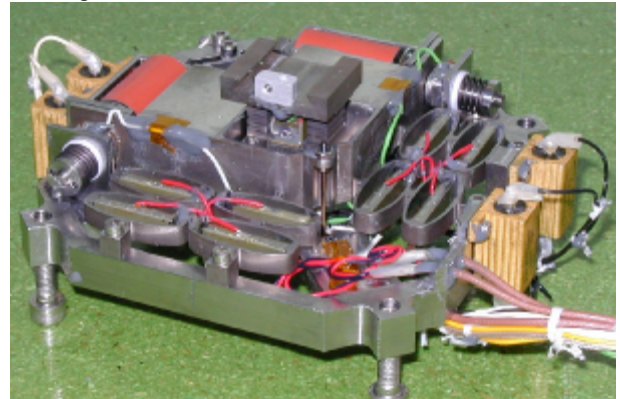


Figure 1 : View of the flight model

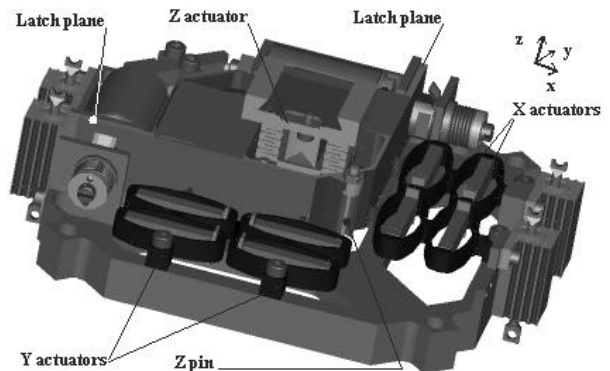


Figure 2 : Basic design of the XY stage

## 2.2 Amplified piezo actuator

To achieve the stroke of 100  $\mu\text{m}$  in a reduced space, several amplified piezo actuators were used. These actuators, initially developed under CNES (French Space Agency) contracts [4] are based on a multilayer piezoelectric components (Figure 3) and a shell which mechanically amplifies the motion and also prestress the piezo components (Figure 4). These actuators are optimised by using a finite element analysis.

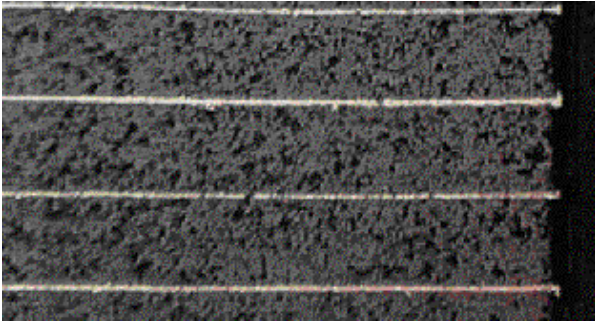


Figure 3 : Cut of view of a multilayer piezoelectric component

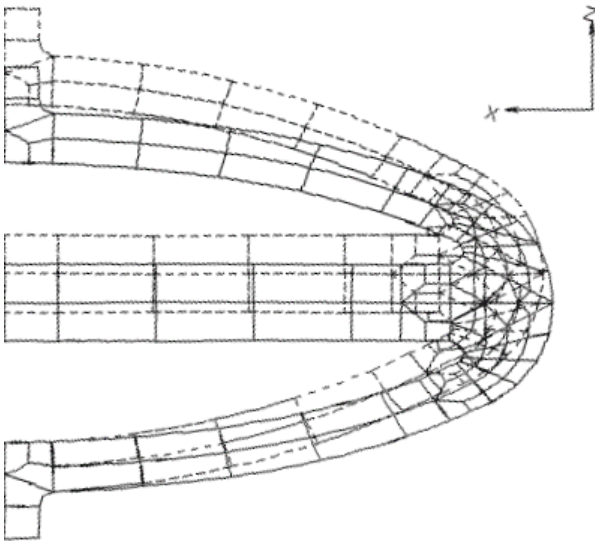


Figure 4 : Finite Element Analysis of the Amplified Piezo Actuator

## 2.3 Guiding and locking philosophies

Because of the high level of vibrations, the XY stage use a latch mechanism. Locking a 2 degrees of freedom parallel mechanism is not straightforward. Two latch planes are implemented to stiffen the X and Y directions. The Z direction is stiffened also by the 2 latch planes and Z pin stiffener, which remains compliant in the X and Y directions (Figure 5).

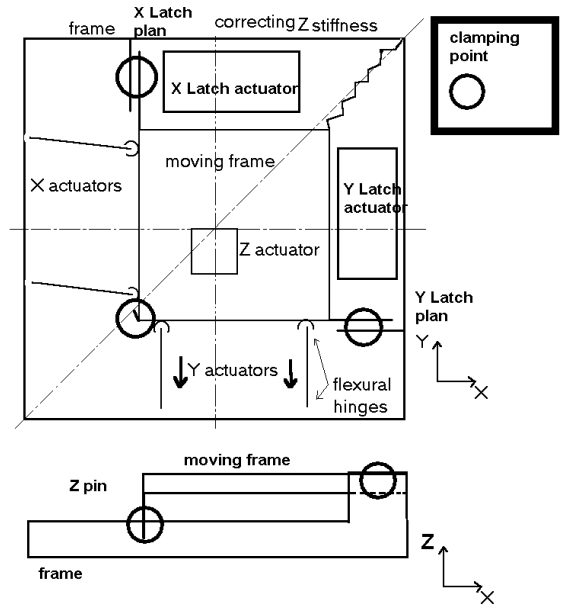


Figure 5 : Guiding and locking principles

The design has been carried out by the extensive use of finite element analysis and CAD software's (Figure 6).

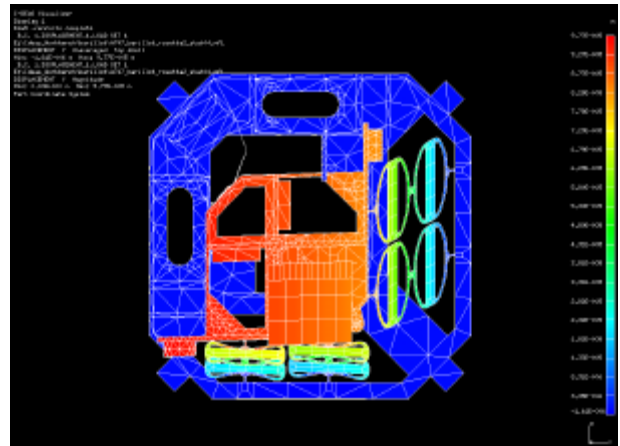


Figure 6 : FEM analysis of the functional behaviour

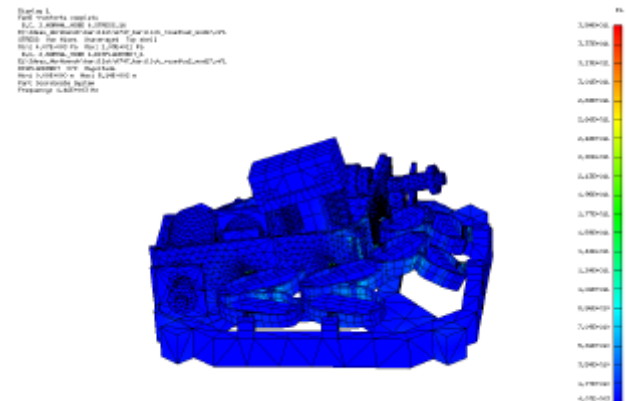


Figure 7 : 1<sup>st</sup> out of plane mode (1460 Hz)

### 3 Functional performances

#### 3.1 Requirements

The functional performances to be achieved are 100  $\mu\text{m}$  of stroke in the X and Y directions, 8  $\mu\text{m}$  in the Z direction, with minimised parasitic rotations :

$$\theta_z < 240 \mu\text{rad},$$
$$\theta_x, \theta_y < 20 \mu\text{rad}.$$

#### 3.2 Testing procedures

The mechanism was tested using a dedicated test bench under class 100, including a laser interferometer. The piezoactuator is then driven at 1 Hz, while the resulting displacement and the position sensor response are monitored (Figure 8, Figure 9). This method is also used to monitor the parasitic out of plane displacements and gives a measurement independent from the drift effect exhibited by the piezo actuator.

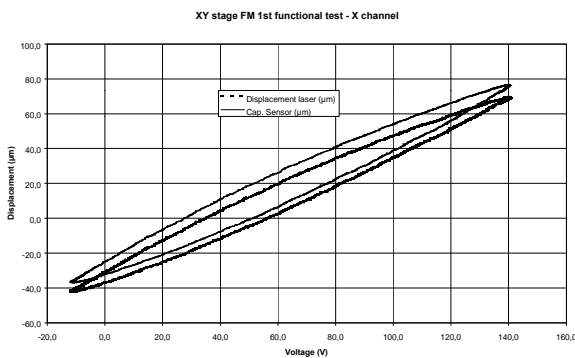


Figure 8 : Measurement of the X axis

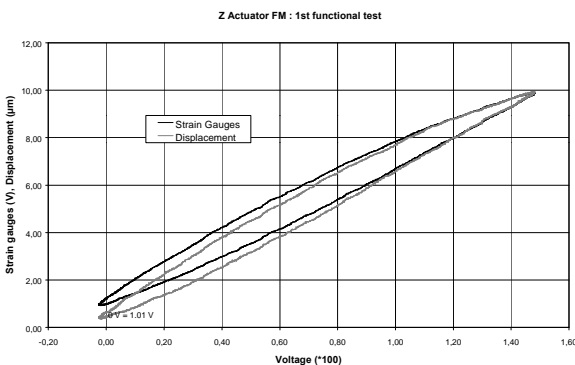


Figure 9 : Measurement of the Z axis

## 4 Latch mechanism

#### 4.1 Design

A review of non explosive actuators (NEA) was performed in 1999 to select a latch mechanism [5]. The flight proven SMA actuator from TiNi aerospace was

selected for its compactness, low shock operation, compatibility with the mass budget and low level of contamination. The basic principle is to use the high strain capability (2 %) of the SMA actuator under heating above 80°C, to break a notched fastener [6].

A latch mechanism was designed including the SMA actuator, a latch status indicator (consisting in two gold electric contacts), a return spring for the broken fastener, a high friction polymer material at the latch plane.

The main points of the latch mechanism are :

- a general novelty of the mechanism due to the used friction plans, because the conventional cup-cone configuration cannot be used due to small clearances,
- although the latch joints are designed quite stiff, the thermo- mechanical and creep effects are small, so that a good margin of preload against vibration loads is obtained,
- very low clearances in the unlocked configuration, which are compatible with the thermo - mechanical behavior of the stage over the whole working temperature range,
- there are two possibilities to break the fastener : pushing or pulling the latch plane. The pushing mode was preferred in order to avoid any creep effect on the latch plane,
- the nut 5 locks the SMA and provides the necessary degree of freedom along the fastener 4 to compensate for the SMA length change (Figure 13),
- a lock force verification procedure was implemented based on the measurement of the change in the fastener length before and after the locking operation. Although the nut 3 is locked with a dynamometer screwdriver and some Braycote EF601 grease is used as lubricant, the locking force exhibit a dispersion of 20% around the nominal value,
- the latch mechanism is completely independent from the stage : it does not interfere with the stage calibration, which has become of main importance during the MIDAS integration.

#### 4.2 Operation results

The latch operation was monitored by a numerical scanner recording the applied voltage, the flowing current, the temperature, the capacitive sensors signals, the latch status indicator signals. A typical chronogram is shown on the Figure 11.

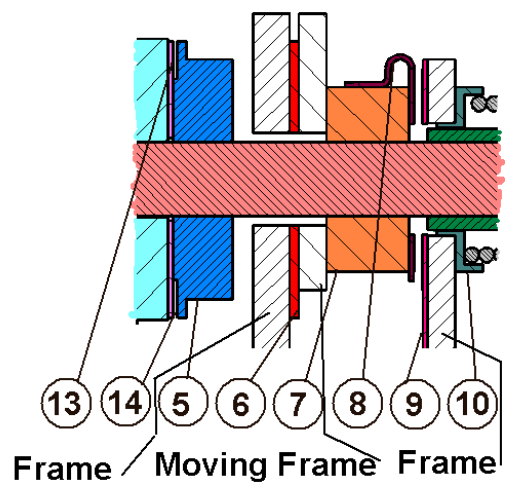
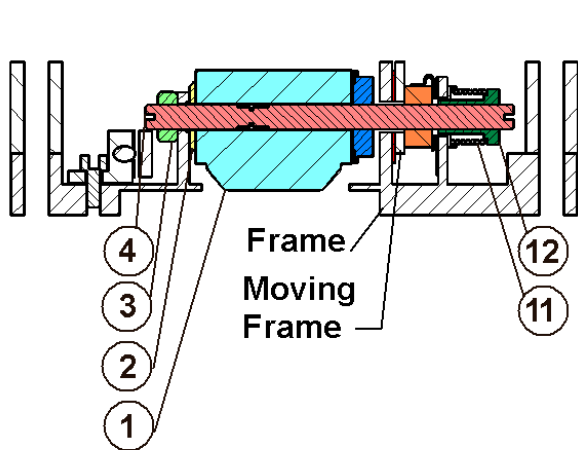


**Figure 10 :** Principle of latch mechanism : a) locked configuration, b) unlocking configuration : 1 : SMA actuator, 2 : washer, 3 : fastener locking nut, 4 : notched fastener, 5 : SMA locking nut, 6 : frictional washer, 7 : nut, 8-9 : latch status indicator, 10 : washer, 11 : fastener return spring, 12 : nut, 13-14 : washers.

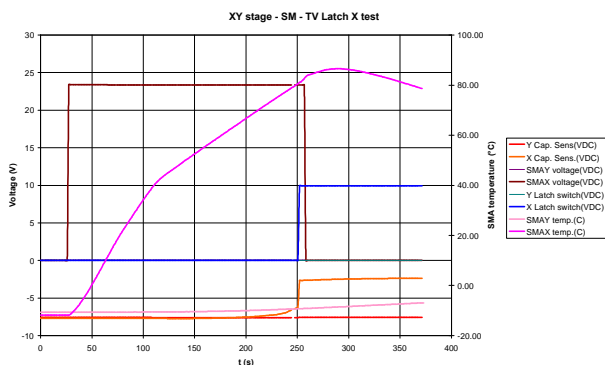


**Figure 11 :** Chronogram of the latch operation under the worst case (-20°C).

The plastic phase can be seen through the capacitive sensor signal. The speed during the notch failure was also monitored using the laser interferometer, showing a speed of around 10 m/s, leading to some rebound effects on the latch status indicator (Figure 12).

More than 20 operations were performed on the same SMA actuators without any loss of performances. The decrease of length (Figure 13) is worth noting and should be taken into account in the design.

The dispersion in the actuation time (for the same external temperature and the same applied power) is around 15 % and is mainly attributed to the locking force dispersion.

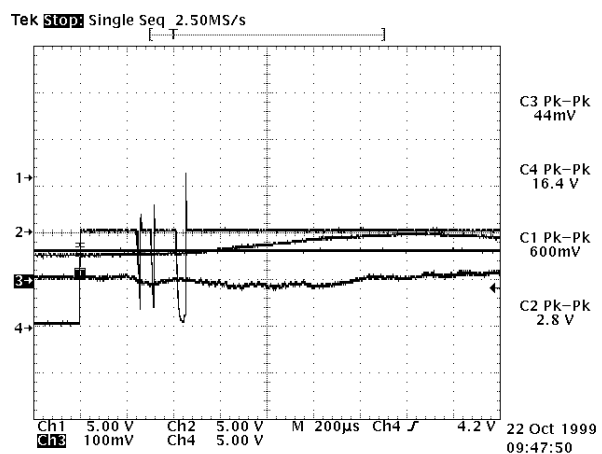


**Figure 12 :** Rebounds on the latch sensor (channel 4)

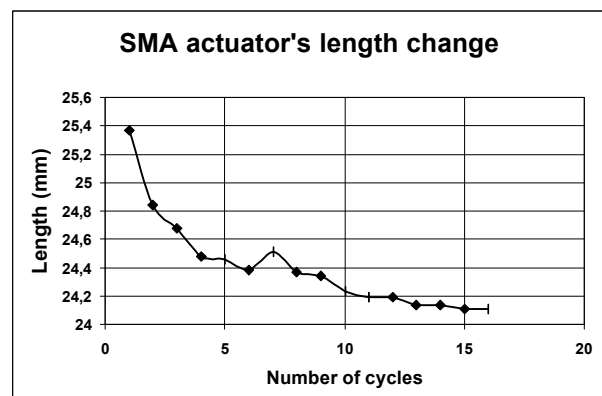


**Figure 13 :** SMA length versus the number of operation

## 5 Qualification campaign

### 5.1 Experimental set – up

The test campaign has used the following equipment's :

- Laser interferometer Polytec OFV3000,
- Impedance analyzer HP4194A,
- Electronic driver CEDRAT LA75A-3,
- Numerical scanner HP34970A,
- TV chamber of CEDRAT,
- EMITECH 26 kN Ling electrodynamic shaker.

### 5.2 Random vibration test

The random vibration test was extremely challenging with a high specified level of 41 grms. It can be seen from the Figure 14 and the Figure 15, that the locked stage behaves in quasistatic up to 1 kHz.

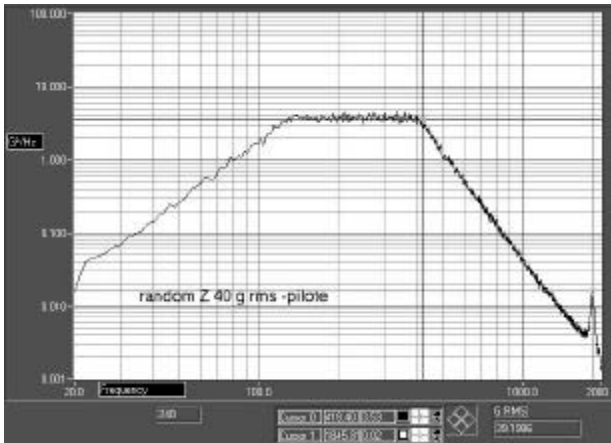


Figure 14 : Random Excitation

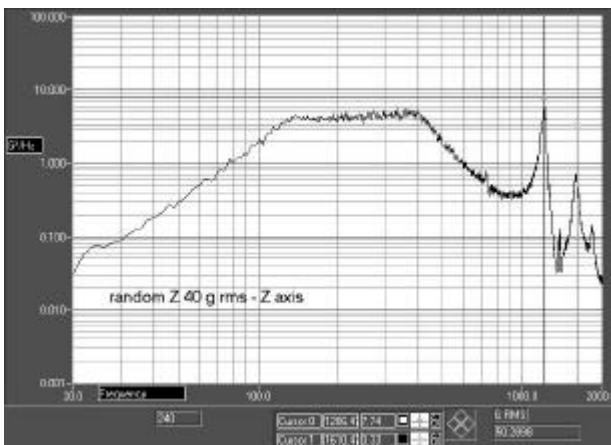


Figure 15 : Resulting level on the Z actuator

		1 <sup>st</sup> sine	10 G	40 G	Final sine
Mode 1	Z act. Y bending	1213	1177	1202	1213
Mode 2	Moving frame Z translation	1350	1359	1350	1360
Mode 3	Z actuator X bending	1504	1502	1514	1511

Table 1 : Change of frequencies during the vibration campaign

### 5.3 Thermal – vacuum test

Several thermal vacuum cycles were performed, both in locked and unlocked configurations, between  $-30^{\circ}\text{C}$  and  $75^{\circ}\text{C}$ . It was first checked that the latch mechanism is able to withstand a storage temperature of  $75^{\circ}\text{C}$  without any faulty operation. Then, the latch mechanism was operated at  $-20^{\circ}\text{C}$  without any problem and with the allowed power budget.

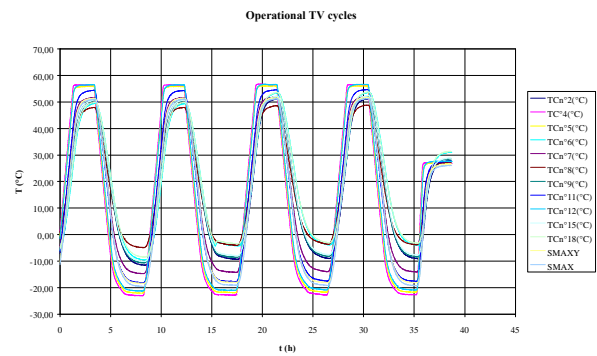


Figure 16 : TV cycles

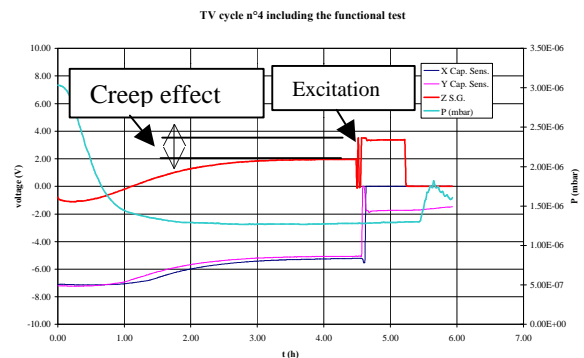


Figure 17 : Thermo-mechanical thermal dependence

One difficult aspect was the correct understanding of the thermo-mechanical behaviour (Figure 17). The piezoelectric material has a low thermal conductivity, leading easily to some thermal gradients. In addition, the piezoelectric thermo-mechanical behaviour is dependent on the electrical connections (eg the behaviour is different if the actuator is closed or open circuited).



## 5.4 Interaction with the latch mechanism

Another aspect is the reverse drift effect exhibited by the piezo actuators under the large pulling force (100 N) in the locked configuration. The pulling force results in a further compression of the piezo material and tends to depole it. This partial depoling can be seen just after the latch operation (Figure 18). Although in closed loop, these aspects disappear, their deep understanding is very useful.

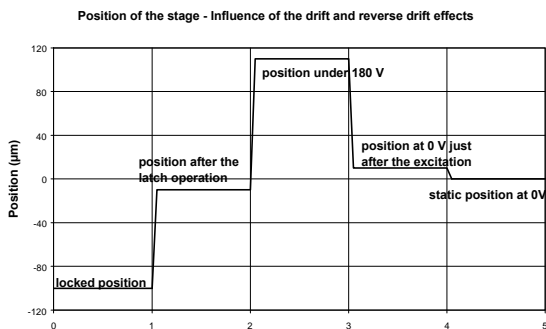


**Figure 18 : Influence of several parameters on the static position.**

## 5.5 Lifetime test

The fatigue effects were tested through a fatigue test of  $10^6$  full stroke cycles, combined with the TV cycles. No problem appeared.

## 6 Calibration activities at the instrument level

### 6.1 Influence of the coarse approach mechanism

Because the stage has not an infinite stiffness, it is sensitive to external forces acting on it [7]. As a result, the static position is also dependent on the position of this mechanism.

### 6.2 Static adjustments

The position of the moving frame was adjusted after its installation in the MIDAS instrument to achieve the situation displayed on the Figure 19. To properly work in closed loop at any temperature, the stage should reach the position between  $-5$  and  $5$  V on the capacitive sensors.

It is therefore critical to have access to the adjustment screws at the instrument level.

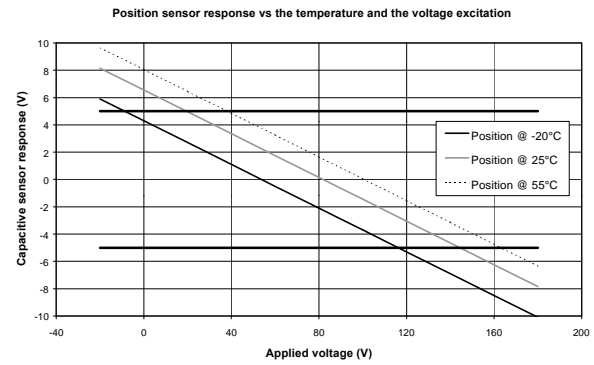


**Figure 19 : Position of the stage depending on the temperature and the voltage excitation.**

## 6.3 Functional results

The environmental tests were repeated at ESA/ESTEC on the QM and the FM instruments. By taking care about the environmental conditions (vibrations), some calibration scans were performed at ESTEC (Figure 20) and illustrate the accuracy capability of a the piezo technology.

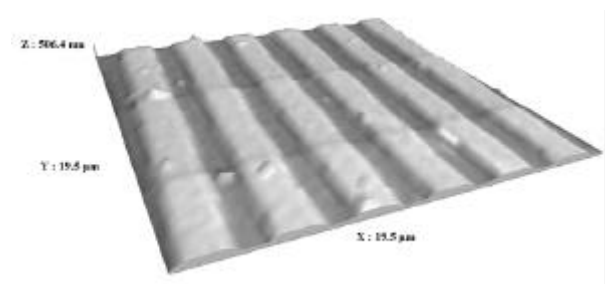


**Figure 20 : Typical scan results – scales in nanometers (courtesy of ESTEC & IWF Graz)**

## 7 Synthesis – Lessons learned

### 7.1 Reproducibility

The same integration and test campaign was performed on 4 identical mechanisms, giving some insight on the reproducibility (Table 2).

The major influence on the XY stage's stroke comes from the components itself, whose properties depends on the fabrication batch.

The lower gain obtained on the last 3 models is explained by the use of the Strain Gauges equipped with a protective layer.

	EQM	QM	FM	FSM
Functional tests XY stage				
Stroke X ( $\mu\text{m}$ )	109.2	115.3	129.4	116.8
Stroke Y ( $\mu\text{m}$ )	107.4	116.9	127.2	114.2
Rz ( $\mu\text{rad}$ )	230	257	239	237
Rx ( $\mu\text{rad}$ )	12	5.5	9.5	3.6
Ry ( $\mu\text{rad}$ )	22	8.1	12.1	5.0
Functional tests Z actuator				
Stroke Z ( $\mu\text{m}$ )	11.1	10.6	11.2	11.7
Strain gauges gain ( $\text{mV}/\mu\text{m}$ )	1.36	1.19	1.17	1.06
Vibration				
1 <sup>st</sup> mode	1213	1163	1206	1180
2 <sup>nd</sup> mode	1504	1437	1468	1430

**Table 2 : Results comparison**

## 7.2 Cable's routing

With 27 interface cables, the cable's routing aspects and its interference's with the MIDAS instruments were underestimated during the development. Both the advises and the help of M. B. Butler have been proved useful. It is advised to include this aspect into the CAD model to further help the integration's documentation.

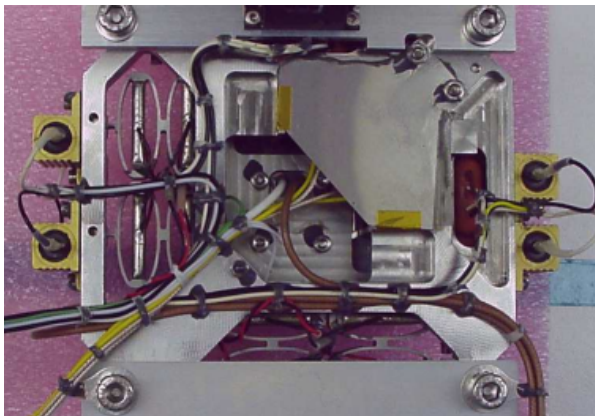


**Figure 21 : View of the cable's routing on the FM**

## 7.3 Position sensors margin

Whilst the stage should have a stroke a 100  $\mu\text{m}$ , the capacitive sensors have a range of reading of about 140  $\mu\text{m}$ . This means that the error on the static position of the moving frame should be lower than 20  $\mu\text{m}$ . This is a serious drawback and one should insure that :

- the thermo-mechanical behavior is compensated by the voltage,
- the stage will not move after 18 months in the locked position and the launch vibrations.

It also explains that some calibration works (static adjustment of the moving frame) have become necessary at the instrument level. Because several effects (thermo-mechanics, drift and reverse drift, gravity) influence this static position, a careful procedure should be used.

It is further advised to keep a sufficient margin for the range of reading of the position sensors.

## 8 Acknowledgements

The authors are grateful to MM. B. Butler, B. Johlander, from ESTEC-SCI/SO, and K. Fritzenwallner, K. Torkar, H. Jeszensky from IWF Graz, for the fruitful discussions during the MIDAS integration.

## 9 References

- [1] J. Romstedt et al., "MIDAS – The first Atomic Force Microscope in space", Proc. of the scanning conference, Monterey (US), 19(3), 142-143, 1997.
- [2] F. Barillot et al., "Design and functional tests of a XY piezoelectric stage for Rosetta/Midas", 8<sup>th</sup> ESMATS Proc., SP438, pp 121-126, 1999.
- [3] CEDRAT Piezo products catalogue, Version 2.1, 2000, Ed. CEDRAT (Meylan), 65 p, [www.cedrat.com](http://www.cedrat.com)
- [4] Le Letty R., Claeysen F., Thomin G., 1997, A new amplified piezoelectric actuator for precise positioning and semi-passive damping, 2<sup>nd</sup> Space Microdynamics & Accurate Control Symp., 389-401.
- [5] M. Lucy et al., "Report on alternatives devices to pyrotechnics on spacecraft", 10th Annual AIAA/USU Conference on Small Satellites, Logan, Utah, September 16-19, 1996.
- [6] Frangibolt® actuator, TiNi Aerospace, [www.tiniaerospace.com](http://www.tiniaerospace.com)
- [7] H. Arends et al., "The MIDAS experiment for the ROSETTA mission", to be presented at the 9<sup>th</sup> ESMATS conference.